Development of III-V Quantum Well and Quantum Dot Solar Cells

Roger E. Welser and Ashok K. Sood
Magnolia Optical Technologies, Inc.
52-B Cummings Park, Suite 314, Woburn, MA 01801

Jay S. Lewis
DARPA/MTO, 675 North Randolph Street,
Arlington, VA 22203

Nibir K. Dhar
Night Vision & Electronics Sensors Directorate,
10221 Burbeck Road, Fort Belvoir, VA 22060

Priyalal Wijewarnasuriya
Army Research Laboratory, 2800 Powder Mill Road,
Adelphi, MD 2078

Roy L. Peters
AQD, US Department of Interior
Sierra Vista, Arizona 85636

Abstract

Nanostructured quantum well and quantum dot solar cells are being widely investigated as a means of extending infrared absorption and enhancing III-V photovoltaic device performance. In the near term, nanostructured solar cell device concepts can potentially be leveraged to improve the performance of multi-junction III-V solar cells for defense and commercial applications. In the long term, nanostructured solar cells provide a pathway to implement advanced photovoltaic device designs which can capture energy typically lost in traditional solar cells.

Introduction

Photovoltaic (PV) devices can provide a mobile source of electrical power for a wide variety of applications in both space and terrestrial environments. Many of these mobile and portable power applications can directly benefit from the development of higher efficiency solar cells. Efficient photovoltaic energy harvesting requires device structures capable of absorbing a wide spectrum of incident radiation and extracting

the photogenerated carriers at high voltages. Nanostructured quantum well and quantum dot absorbers provide a means to extend infrared absorption and enhance III-V photovoltaic device performance. In this paper, we review the status of III-V quantum well and quantum dot solar cell development and the prospects for achieving ultra-high efficiency PV devices.

Pathway for Enhanced III-V Multi-Junction Performance

By stacking multiple p-n junctions of different III-V semiconductor materials into one two-terminal device, multi-junction solar cells have achieved record-high efficiency at converting solar power into electrical power. Under air mass zero (AM0) spectral conditions found in space, InGaP/GaAs/InGaAs inverted metamorphic (IMM) cells have been demonstrated with efficiencies well in excess of 30% [1-2].

Figure 1 compares the simulated current-voltage characteristics of three individual subcells to that of a combined, series-connected IMM multi-junction device. While the current output of the series-connected multi-junction device is limited by the subcell generating the least amount of current, the voltage output is nearly additive. As a result, AM0 efficiencies of greater than 30% can be readily achieved.

To further improve multi-junction performance, several groups have explored adding nanostructured regions to one or more of the subcells [3-5]. By boosting current collection in the middle subcell, such an approach can result in better current matching, enabling multi-junction devices with a higher current density. In some of the best III-V nanostructured solar cells reported to date, both the short circuit current density and overall efficiency exceeds that of GaAs reference devices without the nanostructured absorbers [6-7].
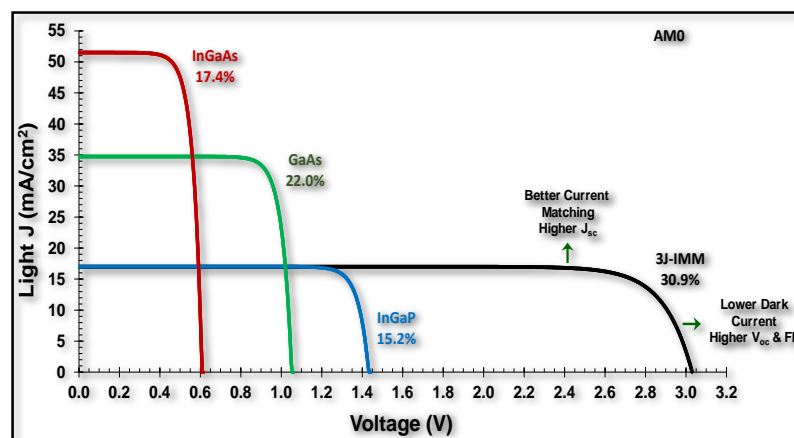

Figure 1: Simulated AM0 illuminated current-voltage characteristics of conventional III-V solar cells, both as individual single-junction devices and as a series-connected, three-junction inverted metamorphic (3J-IMM) device. The potential impact of incorporating nanostructured absorber designs is also highlighted.

Nanostructured absorbers have also been associated with improved radiation resistance [8]. Alternatively, as will be discussed later in more detail, nanostructured absorbers can also be employed as part of a more general band gap engineering approach to improve the voltage and fill factor performance of the individual subcells, and ultimately of the multi-junction device. The arrows in Figure 1 illustrate the potential impact nanostructured absorbers can have on the illuminated current-voltage characteristics of an IMM device.

Limitations of III-V Multi-Junction Architecture

III-V IMM multi-junction devices have achieved even higher efficiencies under an air mass spectrum (AM1.5) typically used to characterize terrestrial performance – efficiencies that can exceed 35% at 1-sun and 40% under concentration [9-10]. However, changes in the solar spectrum can dramatically degrade the performance of multi-junction devices – changes that occur naturally throughout the day, from season to season, and from location to location as sunlight passes through the earth's atmosphere. As illustrated in Figure 2, the efficiency of a multi-junction device will decrease by more than a factor of two under higher air mass spectra.
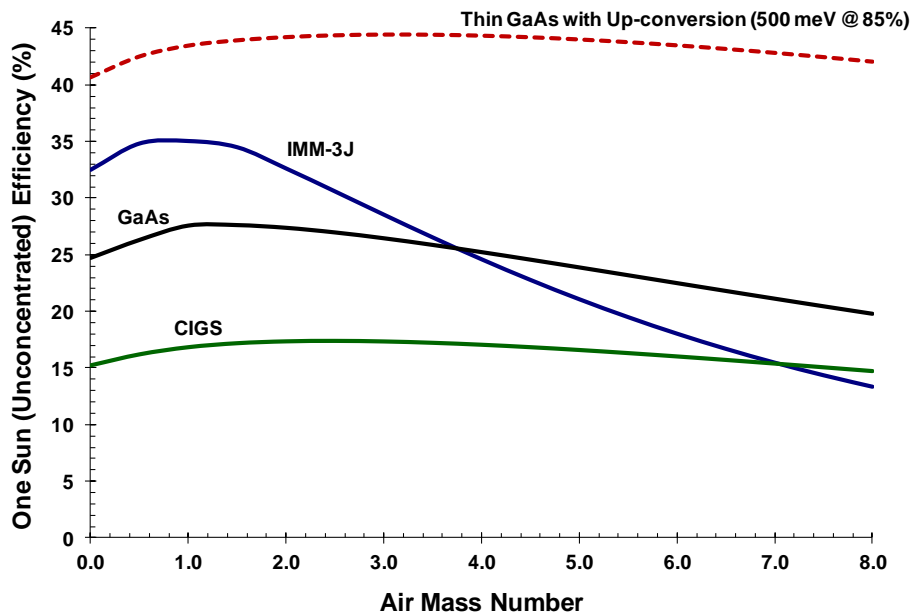
Figure 2: Projected un-concentrated efficiency versus air mass spectrum for several different types of solar cell structures, including a high-performance IMM triple-junction III-V structure, a single-junction CIGS cell, and a single-junction GaAs solar cell. Also shown is the theoretical performance of a thin GaAs-based device incorporating up-converting and light-trapping structures to harness a notable fraction of the available low energy photons. The calculations assume a Bird-Riordan model of the air mass spectrums and realistic spectral response and dark diode characteristics, as detailed in reference [13].

The reduction in efficiency is due to a decrease in the current output of the series-connected multi-junction device, which is limited by the subcell generating the least amount of photocurrent. Series-connected multi-junction cells can also degrade more rapidly than single-junction III-V cells upon irradiation, particularly as the current output of the limiting subcell fails. Moreover, multi-junction III-V cells require thick, complex epitaxial layers and are therefore inherently expensive to manufacture.

Thus the inconsistent performance under changing environmental conditions and high manufacturing costs of multi-junction III-V cells severely hampers the application of this established high-efficiency technology.

Thin-film single-junction III-V cells can potentially address the performance and cost limitations of multi-junction devices. By avoiding current-matching constraints, single-junction structures can offer a more robust performance than multi-junction devices. The efficiency of established single-junction CIGS and GaAs cell technologies is more stable to changes in the incident spectrum, and can actually outperform III-V multi-junction structures under higher air mass spectrums, as depicted in Figure 2.

Moreover, the efficiency of single-junction III-V cells can be dramatically increased by employing additional structures that leverage optical up-conversion and/or hot carrier effects. Theoretically, both up-conversion and hot carrier mechanisms have been projected to increase the limiting one-sun efficiency of single-junction photovoltaic devices to over 50% [11-12]. By combining thin III-V absorber structures with advanced light-trapping structures, nano-enhanced III-V single-junction devices can potentially deliver high-efficiency performance in a flexible format at a fraction of the cost of multi-junction structures. As illustrated in Figure 2, unconcentrated efficiencies of more than 40% over a wide range of spectrums are projected for an optically-thin GaAs-based device that can harness 85% of the infrared photons falling within 500 meV of the GaAs band edge [13].

III-V Nanostructured Intermediate Band Solar Cells

In many research studies reported in the literature, III-V nanostructured absorbers are employed to generate an intermediate band which can potentially increase photovoltaic efficiency by up-converting sub-band gap photons [14]. By forming an intermediate band in a single-junction photovoltaic cell, the energy conversion efficiency of the cell can potentially be dramatically enhanced. An enhancement in efficiency is projected when infrared light absorption is increased via optical up-conversion to minimize optical transmission losses. This type of internally up-converting photovoltaic device is known as an intermediate band solar cell (IBSC).

Figure 3 (a) shows the band diagram of a photovoltaic cell with an intermediate band. This configuration enables the absorption of two additional sub-bandgap photons in addition to one-above bandgap photon. With proper design, the limiting open circuit

(a)   **(b)**
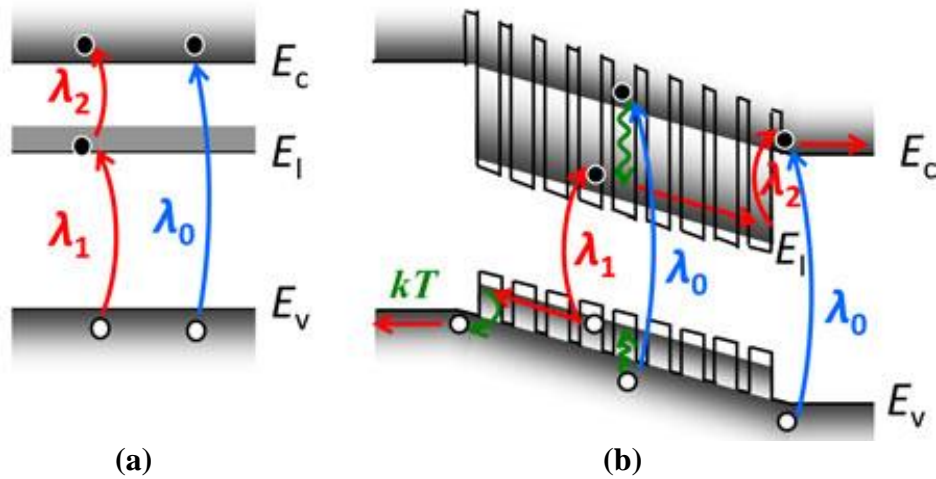
Figure 3: Schematic depictions comparing a two-step sequential up-conversion process via an intermediate band to conventional band-to-band absorption in (a) an idealized setting and (b) as part of a multi-layered nanostructured absorber. See reference [16] for details.

voltage should not be affected by the insertion of the intermediate band. Instead, the open circuit voltage will be equal to the separation between valance and conduction band quasi Fermi levels of the wider bandgap host material, independent of the intermediate band material. An ideal IBSC thus increases current output without degrading voltage, e.g. the IB is electrically isolated and does not emit photons. Based on detailed balance IBSC theory, a maximum efficiency is possible when the host material bandgap is 1.95 eV with an intermediate band located 0.71 eV above the valence band [12, 14].

For an IBSC to work properly, the nanostructured material system being used must satisfy certain conditions in terms of bandgaps and band alignments [15]. Many attempts have been made to realize IBSCs based upon quantum dot and quantum well nanostructures. Frequently, nanostructured systems combining InAs, InGaAs, and GaSb narrow band gap material with GaAs as a host material have been studied. Figure 3 (b) depicts both conventional and intermediate band absorption processes in a GaAs-based multi-layered nanostructured absorber. Both quantum dot and quantum well GaAs-based IBSC devices have successfully demonstrated sequential up-conversion, but are at least partially emitting, thus degrading their voltage performance [16].

Ongoing efforts in the field of nanostructured IBSCs are focused on better understanding the limitations on voltage output, maximizing current generation, and developing exotic material combinations with more ideal band alignments for IBSC devices [17-20]. For example, Figure 4 (a) shows the schematic of an InAs quantum dot (QD) device employing a GaAs, GaAsSb, and AlAsSb cladding layer scheme. This III-V material system has near ideal bandgaps for IBSCs, and furthermore,

InAs(Sb)/AlAsSb QDs exhibit a type II band alignment. This offers strong electron confinement, while the valence band offset at the InAs(Sb)/AlAsSb interface is small (zero for certain As and Sb compositions).

Figure 4 (b) shows the atomic force microscope image of InAs/AlAsSb QDs with 5 ML of GaAs below the QDs. These QDs have an areal density 2×10^{10} cm^{-2} and are 4.1 nm tall and 33 nm in diameter. The average size of these QDs can be easily controlled, and hence the energies of the quantum confined states, simply by changing the InAs coverage. Power-dependent photoluminescence measurements on these QD samples confirm a type II band alignment [20]. In samples containing GaAs/InAs/GaAsSb QDs, carrier lifetimes as long as 7 ns are measured. This is greater than the lifetimes measured in typical type I QD systems. These longer lifetimes are especially beneficial for efficient carrier extraction, leading to higher IBSC efficiency.

To understand the performance and operation of InAs/AlAsSb QD PV cells, an AlAsSb p-i-n solar cell device has been fabricated with 10 layers of InAs QDs buried within cladding layers similar to the schematic in Figure 4 (a). EQE data from an AlAsSb control cell without dots or cladding layers and another cell with cladding layers only is presented for comparison in Figure 5. The EQE spectra show an extended wavelength response in cases where there are cladding layers and QDs. To date, this is one of the longest wavelength responses reported in any QD PV device [20]. The QD cell shows an extremely broad-band photoresponse up to 1800 nm,

(a)   **(b)**
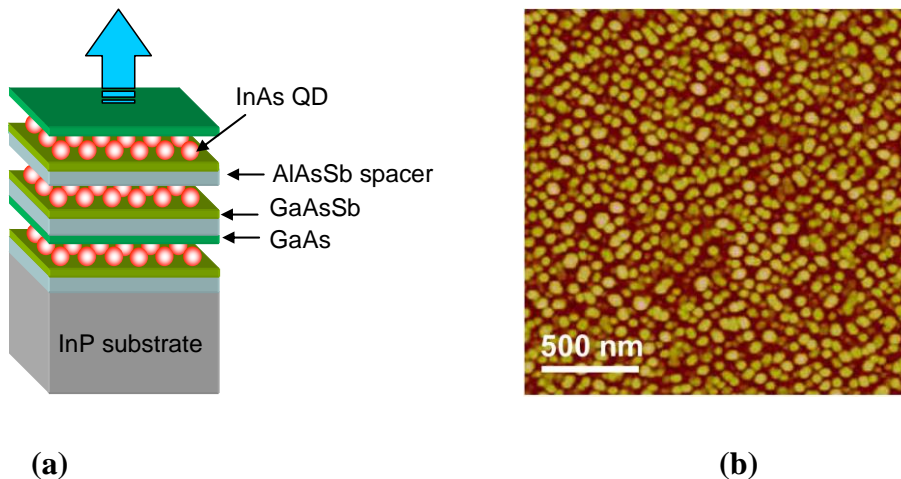
Figure 4 (a): Schematic of an InAs QD structure with GaAs and GaAs$_{0.95}$Sb$_{0.05}$ cladding layers, as well as thin AlAsSb spacers, and (b) atomic force microscopy image of InAs QDs on AlAs$_{0.56}$Sb$_{0.44}$ with a five-monolayer-thick GaAs cladding layer placed beneath the QDs [19].
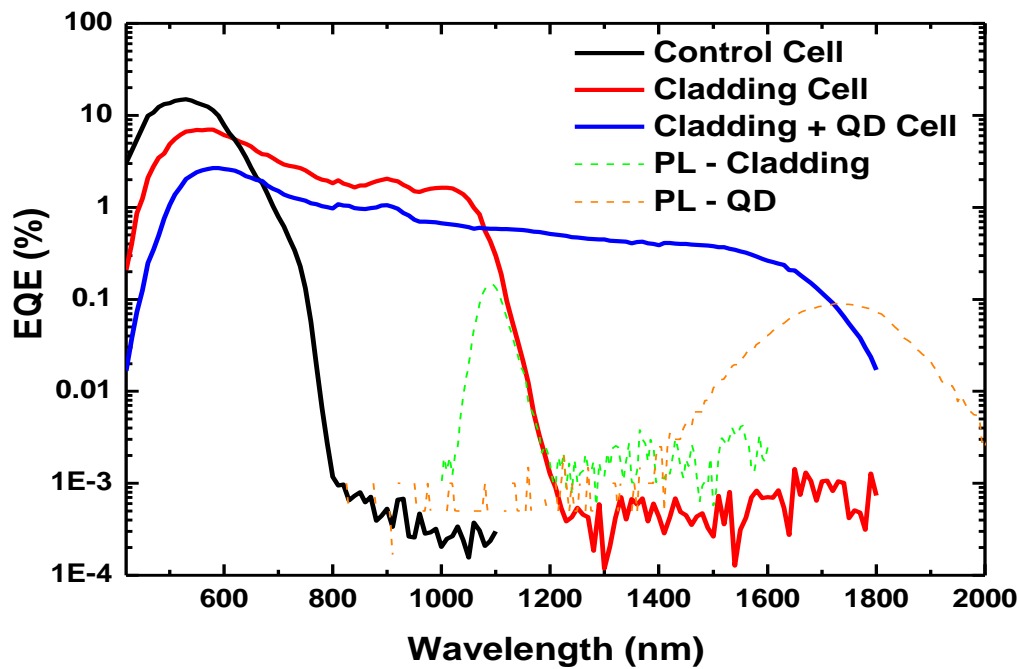
Figure 5 External quantum efficiency measured from an InAs/AlAsSb QD PV cell with GaAs and GaAsSb cladding layers, compared to measurements from a control cell and a cell incorporating only the cladding layers (no QDs) [20].

consistent with the PL measured from respective devices. Though these results are encouraging, further device optimization will be required to achieve a high efficiency IBSC performance, perhaps including the use of high solar concentrations.

III-V Nanostructured Hot Carrier Solar Cells

In parallel to the ongoing work on III-V nanostructured IBSC devices, III-V quantum well structures have also been explored as a means to enhance hot carrier extraction and increase photovoltaic efficiency by boosting the limiting voltage output [21-22]. Hot carrier solar cells (HCSCs) seek to harness above-bandgap photon energy typically lost as heat by extracting hot photo-generated carriers before they thermalize down to the absorber band gap – see Figure 6 (a).

Ideally a HCSC would employ a highly selective energy contact, increasing the device voltage while maintaining the current output. However, theoretical work by Le Bris and Guillemoles suggests that performance benefits can still be obtained when employing a semi-selective contact [23]. Figure 6 (b) depicts the photon-induced generation of a hot carrier population within a potential barrier formed when a narrow energy-gap well is embedded within a higher-energy gap matrix. If the hot carriers can be extracted from the well before thermalizing, a photovoltaic power conversion efficiency of 50% could be obtained. Recent approaches to maintaining the hot carrier

(a)   **(b)**
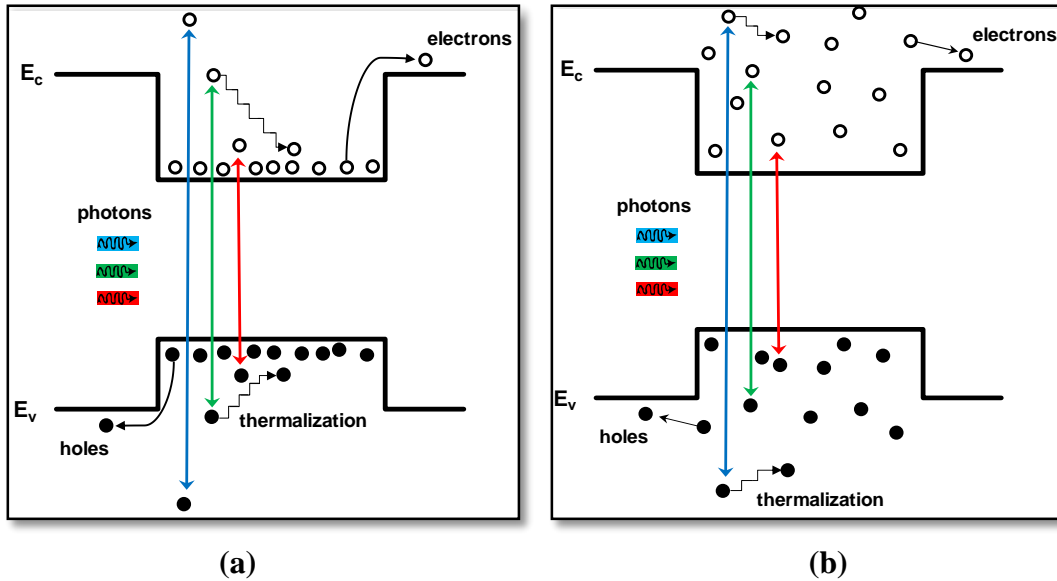
Figure 6: Schematic depiction of (a) conventional thermalization losses and thermal escape processes, and (b) generation and extraction of hot carriers from a potential well.

population necessary for demonstrating HCSC performance have included exploring high concentration operation and employing type-II heterostructures to inhibit radiative recombination [24-25]. Engineering the compositional profile of the wells has also been reported to suppress radiative recombination [20], as will be detailed later, and may indicate enhanced hot carrier extraction.

High-Voltage III-V Quantum Well Solar Cells

Nanostructured materials are enabling new device concepts that can radically enhance the operation of traditional semiconductor structures. Nanostructured solar cell structures in particular seek to harness a wide spectrum of photons at higher voltages by embedding low energy-gap wells or dots within a high energy-gap matrix. While previous work in the area of quantum well and quantum dot solar cells has frequently resulted in subpar voltage performance, Magnolia has developed a unique extended emitter heterojunction device structure based upon the quantum solar cell concept to achieve high-voltage operation by reducing the dark diode current [26].

Figure 7 depicts an example of Magnolia's general band-gap engineering approach for demonstrating high-voltage quantum well photovoltaic devices. In this example, the baseline material structure consists of an N-on-P structure utilizing an AlInP window layer and an extended wide band gap InGaP/AlGaAs emitter structure. AlGaAs alloys are also used for the back surface field (BSF) and transparent back contact layers. Employing an extended type II InGaP emitter / AlGaAs barrier heterostructure provides a means of reducing both non-radiative n=1 diffusion and n=2 space charge recombination components of the diode dark current. The use of
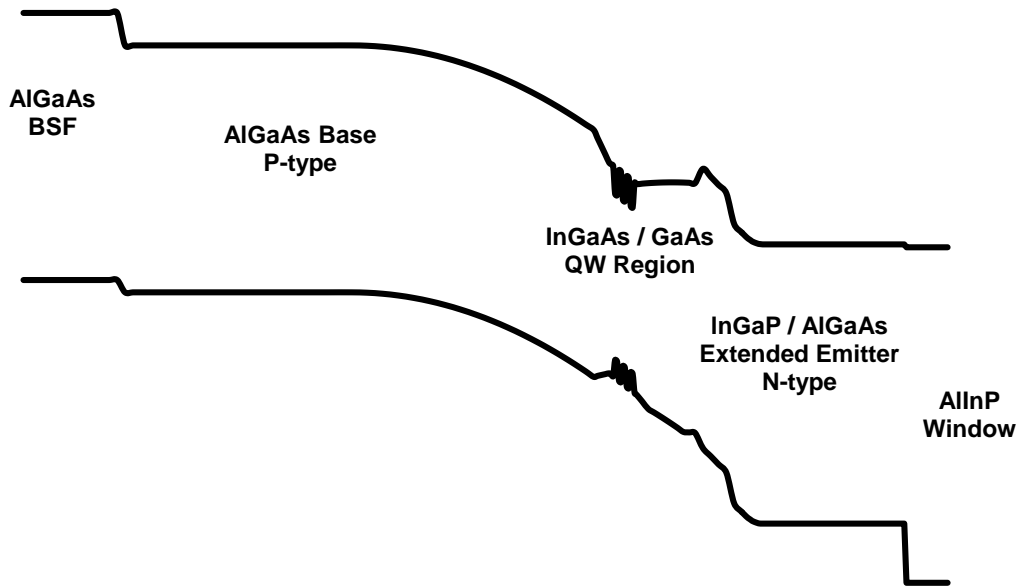
Figure 7: Simplified band structure of an n-type emitter / p-type base multiple InGaAs quantum well solar cell structure employing an extended wide band gap emitter in order to minimize non-radiative dark current mechanisms.

wide band gap material can minimize the dark current and hence increase the operating voltage of a photovoltaic device, increasing the average energy-gap of the absorber can also reduce its current generating capabilities.

To compensate for the loss in absorption due to the wide band gap material, an InGaAs / GaAs quantum well structure is inserted into the junction depletion region of the p-type AlGaAs base layer to extend the absorption profile further into the infrared. By judiciously combining wide and narrow energy-gap material, this general band-gap engineering approach can potentially improve voltage and fill-factor performance without sacrificing the current output.

High-voltage InGaAs quantum well devices with one-sun open circuit voltages greater than 1 V have been demonstrated by utilizing structures that employ advanced band gap engineering to suppress non-radiative recombination and expose the limiting radiative component of the diode current. Figure 8 compares the current-voltage characteristics from a high-voltage single-junction GaAs-based device employing an extended heterostructure with InGaAs wells to a conventional device structure. The combined InGaAs quantum well / extended wide band-gap emitter structure has nearly the same current output as the standard structure ($J_{sc} \sim 16$ mA/cm^2), but a higher open-circuit voltage ($V_{oc} \sim 1.05$ V) and fill factor (FF $\sim 84.5\%$) [26].

The underlying dark diode characteristics of these devices have been assessed by measuring the light I-V characteristics under variable illumination intensities and fitting the resulting J_{sc}-V_{oc} data with a simple two-diode model [26-27]. The
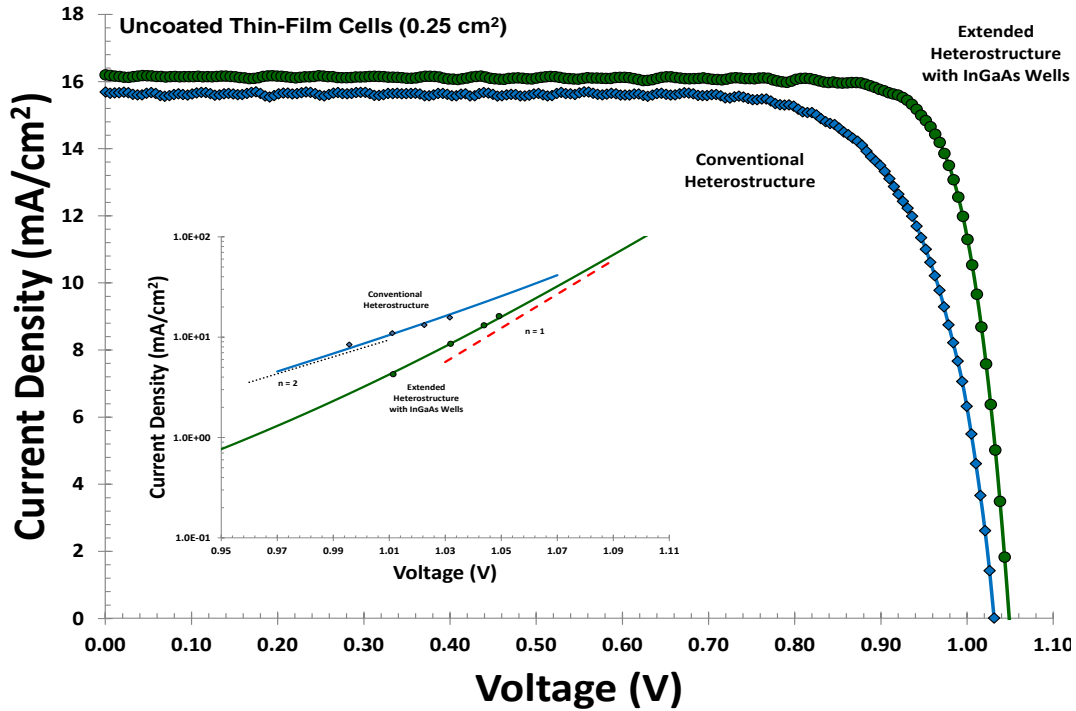
Figure 8: One-sun light I-V curves from a high-voltage single-junction GaAs-based device employing an extended heterostructure with InGaAs quantum wells compared to a conventional device structure. A comparison of the dark diode characteristics is also shown inset. Data taken from small area (0.25 cm^2) uncoated test cells [26].

combined InGaAs quantum well / extended wide band-gap emitter structure has both a lower and more ideal dark diode current, consistent with the observed increase in V_{oc} and FF.

In the near term, a general band-gap engineering approach combining both narrow and wide band gap material can be employed to improve multi-junction performance by lowering the dark diode current in each of the individual subcells of a multi-junction structure. Such an approach could also be coupled with advanced light trapping structures to realize lower-cost, high-performance single-junction devices capable of maintaining their performance over a wider range of operating conditions. Longer term, these high-voltage GaAs-based nanostructured devices could be further optimized to harness hot carrier and intermediate band up-conversion processes to achieve ultra-high efficiency performance, as will be further discussed in the next section.

## Inhibition of Radiative Recombination in Step-Graded Wells

Several reports in the literature over the past decade indicate that it may be possible to inhibit radiative recombination in III-V nanostructured absorbers by manipulating the compositional profile of the individual quantum wells [28-32]. In particular, observations of reduced photoluminescence emission intensity have been reported in step-graded wells relative to conventional square wells [28,32]. However, for a photovoltaic device to benefit from a reduction in radiative recombination, non-radiative recombination must be sufficiently suppressed. By inserting both square and step-graded wells into high-voltage structures similar to those described in the previous section, reductions in the diode dark current have also recently been observed [20].

Figure 9 compares the photoluminescence (PL) emissions from two sets of single-well high-voltage photovoltaic devices. Figure 9 (a) overlays the normalized PL spectrum from a set of square well InGaAs quantum well solar cells with varying well thickness in which the indium composition in the well has been adjusted to maintain a peak PL emission of 1.32 eV. Figure 9 (b) compares the PL spectrum from two similar step-graded well devices with different well thickness in which the indium composition in the well has again been adjusted to maintain a peak PL emission of 1.32 eV.

The normalized PL intensity from the square InGaAs wells clearly decreases as the well thickness decreases from 30 nm to 15 nm, but is only marginally lower for the structure with the thinnest well (2.5 nm), consistent with a transition from a three-dimensional (3D) to a two-dimensional (2D) density of states [20]. The normalized PL intensity from the step-graded InGaAs wells also shows a thickness dependence, and is lower in overall intensity than the square wells of comparable total thickness.

As seen in Figure 10, the n=1 reverse saturation current density (J_{o1}) extracted from two-diode fits of the measured dark diode current from these same sets of high-voltage quantum well solar cells shows the same thickness dependence as the PL spectrums in Figure 9. For thicker square-well samples, the variation in J_{o1} with well thickness is well fit by a 3D representation of the radiative current density [20]. On the other hand, for thinner square-well samples, the variation in J_{o1} with well thickness is well fit by a 2D representation of the radiative current density. Meanwhile, the variation in J_{o1} with well thickness of the step-graded wells follows a 3D dependence that is significantly lower than the comparable square-well structures. The apparent radiative recombination coefficient of the step-graded structures is over 3x lower than the square structures with a comparable effective well energy of 1.32 eV.

There are several possible mechanisms by which a step-graded well profile or other device designs may reduce the effective radiative recombination coefficient of emissions from the well region, and thus enhance the limiting operating voltage of
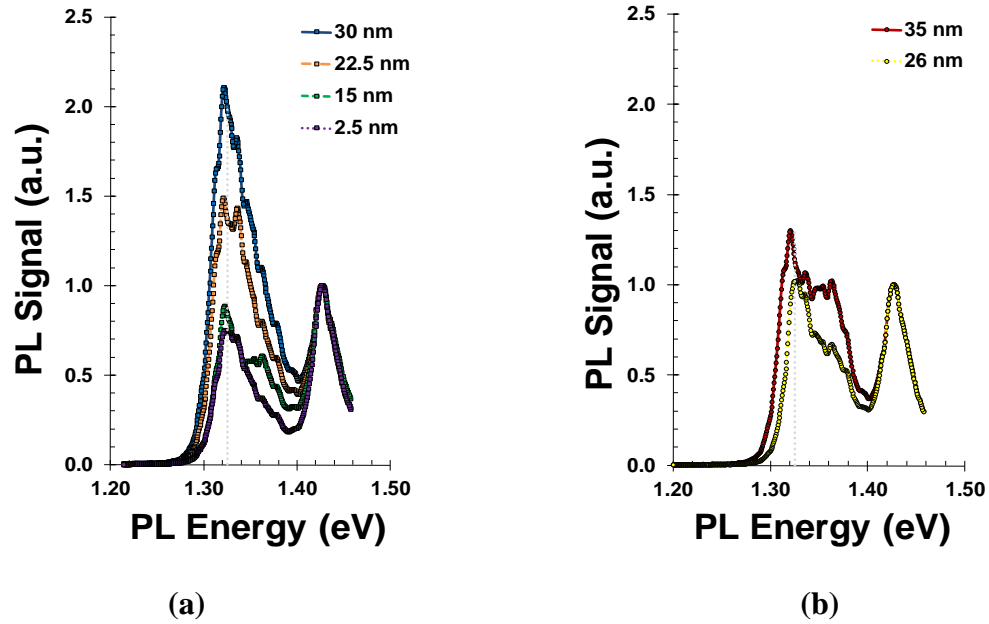
Figure 9: Normalized photoluminescence spectra from two different sets of as-grown QWSC structures employing (a) single square InGaAs wells and (b) single step-graded InGaAs wells. The PL emissions were generated with excitation from a 785 nm laser source; the PL intensity measured on each sample has been normalized to the peak GaAs base layer emissions near 1.42 eV.
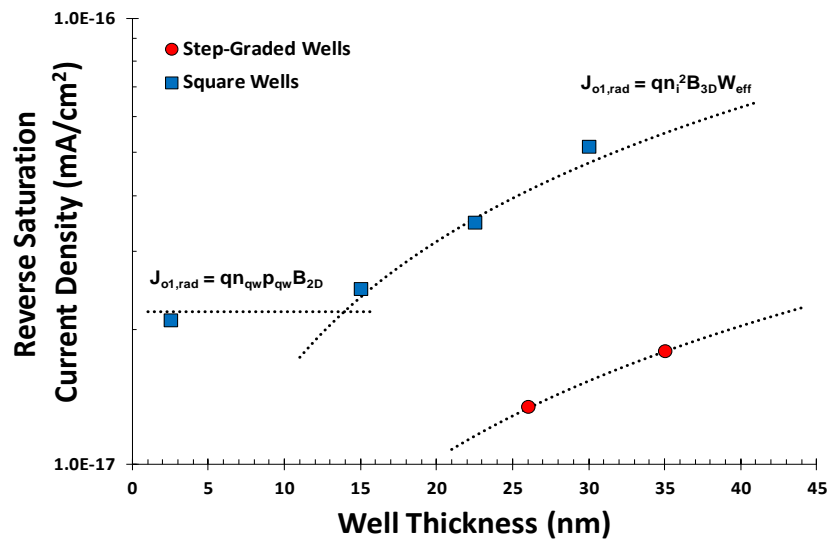
Figure 10: Reverse saturation current density of the n=1 component of the diode current as derived from the measured dark diode current in square (square shapes) and step-graded (circles) InGaAs well structures. All the structures have a peak PL emission from the well near 1.32 eV. Also shown is the expected variation in the radiative dark current in both the three-dimensional (3D) and two-dimensional (2D) regimes.
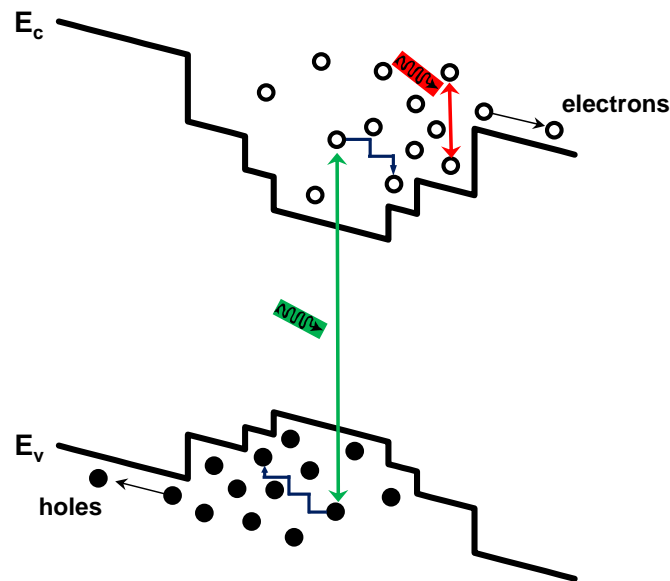
Figure 11: Illustration of field- and photon-assisted spatial separation of hot carriers into wider energy-gap material in a compositionally step-graded well.

photovoltaic devices. Some of the earliest work on step-graded well solar cell structures focused on faster thermal escape processes that could allow photogenerated carriers to readily hop out of the well [29-31]. Shifts in the absorption profile or a restriction in the angular emissions could also lead to a reduction in radiative emissions. However, previous analysis suggests these mechanisms are not likely playing a significant role [20]. Instead, more recent investigations suggest that enhanced extraction of hot carriers from the well region could provide a better explanation for the inhibited radiative recombination observed in the step-graded structures, as illustrated in Figure 11.

In particular, Figure 11 illustrates both photon- and field-assisted spatial separation of hot carriers into wider energy-gap material in a compositionally step-grade well. In brief, if photogenerated carriers can be pushed into the wider energy-gap material faster than they can thermalize, aided by the pull of a built-in electrical field and/or the sequential absorption of an infrared photon, the "hot energy" of photons absorbed in the well can be effectively harnessed to suppress radiative recombination and increase photovoltaic conversion efficiency. Recent theoretical work suggests that a new type of device, an intermediate-band-assisted hot-carrier solar cell, could solve serious issues associated with both IBSCs and HCSCs [33]. A step-graded well structure could represent a practical realization of this theoretical hot-carrier device, and could be a focus on subsequent development work in the area of nanostructured III-V solar cells.

Conclusions

Nanostructured quantum well and quantum dot solar cells are being widely investigated as a means of extending infrared absorption and enhancing III-V photovoltaic device performance. In some of the best III-V nanostructured solar cells reported to date, both the short circuit current density and overall efficiency exceeds that of GaAs reference devices without the nanostructured absorbers. In the near term, such nanostructured solar cell device concepts can potentially be leveraged to improve the performance of multi-junction III-V solar cells routinely employed for space power applications.

In the long term, nanostructured solar cells provide a pathway to implement advanced photovoltaic device designs which can capture energy typically lost in traditional devices. In particular, a compositional step-grade design has been experimentally observed to enhance the performance of high-voltage InGaAs quantum well solar cells by reducing the overall diode dark current, and may provide a pathway for harnessing both intermediate-band absorption and hot carrier extraction processes.

References

[1]   P. Patel, D. Aiken, A. Boca, B. Cho, D. Chumney, M. B. Clevenger, A. Cornfeld, N. Fatemi, Y. Lin, J. McCarty, F. Newman, P. Sharps, J. Spann, M. Stan, J. Steinfeldt, C. Strautin, and T. Varghese, "Experimental Results From Performance Improvement and Radiation Hardening of Inverted Metamorphic Multijunction Solar Cells," IEEE J. of Photovoltaics 2, 377 - 381 (July 2012).

[2]   J. Boisvert, D. Law, R. King, E. Rehder, P. Chiu, D. Bhusari, C. Fetzer, X. Liu, W. Hong S. Mesropian, R. Woo, K. Edmondson, H. Cotal, D. Krut, S. Singer, S. Wierman, and N. H. Karam, "High Efficiency Inverted Metamorphic (IMM) Solar Cells," Proceedings of 39th IEEE PVSC Conference, Tampa, 2790 - 2792 (June 2013).

[3]   R. P. Raffaelle, S. Sinharoy, J. Andersen, D. Wilt, and S.G. Bailey, "Multi-junction Solar Cell Spectral Tuning with Quantum Dots," Proc. of 4th IEEE WCPEC, pp. 162-166 (May 2006).

[4]   S. Fafard, "Solar Cell with Epitaxially Grown Quantum Dot Material," US Patent # 7,863,516 (January 2011).

[5]   C. Kerestes, S. Polly, D. Forbes, C. Bailey, A. Podell, J. Spann, P. Patel, B. Richards, P. Sharps, S. Hubbard, "Fabrication and Analysis of Multijunction Solar Cells with a Quantum Dot (In) GaAs Junction," Prog. Photovolt: Res. Appl. 22, 1172-1179 (November 2014).

[6]   C. G. Bailey, D. V. Forbes, S. J. Polly, Z. Bittner, Y. Dai, C. Marckos, R. P. Raffaelle, and S. M. Hubbard, "Open-Circuit Voltage Improvement of InAs/GaAs Quantum-Dot Solar Cells Using Reduced InAs Coverage," IEEE J. of Photovoltaics, vol. 2, pp. 269-275 (July 2012).

[7] H. Fujii, K. Toprasertpong, Y. Wang, K. Watanabe, M. Sugiyama, and Y. Nakano, "100-Period, 1.23eV BandgapInGaAs/GaAsP Quantum Wells for High-Efficiency GaAs Solar Cells: Toward Current-Matched Ge-Based Tandem Cells," Prog. Photovolt: Res. Appl. 221, 784-795 (December 2013).

[8] C. D. Cress, S. M. Hubbard, B. J. Landi, R. P. Raffaelle, D. M. Wilt, "Quantum Dot Solar Cell Tolerance to Alpha-Particle Irradiation," Appl. Phys. Lett. 91, 183108 (October 2007).

[9] M. A. Green, K. Emery, Y. Hishikawa, W. Warta and E. D. Dunlop, "Solar cell efficiency tables (Version 45)," Prog. Photovolt: Res. Appl. 23, 1-9 (December 2014).

[10] http://www.nrel.gov/ncpv/images/efficiency_chart.jpg

[11] T. Trupke, M. A. Green, and P. Wurfel, "Improving Solar Cell Efficiency by Up-Conversion of Sub-Band-Gap Light," J. Applied Phys. 92, 4117-4122 (October 2002).

[12] P. Wurfel, A. S. Brown, T. E. Humphrey, and M. A. Green "Particle Conservation in the Hot-Carrier Solar Cell," Prog. Photovolt: Res. Appl. 13, 277-285 (February 2005).

[13] R. E. Welser, G. G. Pethuraja, J. W. Zeller, A. K. Sood, K. A. Sablon, S. R. Tatavarti, and N. K. Dhar, "High-Voltage Thin-Absorber Photovoltaic Device Structures for Efficient Energy Harvesting," Proc. of SPIE, vol. 9115, no. 91150F (May 2014).

[14] A. Luque, A. Marti, and C. Stanley, "Understanding Intermediate Band Solar Cells," Nature Photonics, vol. 6, pp 146-152 (March 2012).

[15] M. Y. Levy, C. Honsberg, A. Martí, and A. Luque, "Quantum Dot Intermediate Band Solar Cell Material Systems with Negligible Valence Band Offsets," IEEE 31st Photovoltaic Specialists Conference, pp. 90-93 (2005).

[16] M. Sugiyama, Y. Wang, K. Watanabe, T. Morioka, Y. Okada, and Y. Nakano, "Photocurrent Generation by Two-Step Photon Absorption with Quantum-Well Superlattice Cell," IEEE J. Photovoltaics 2, 298-302 (July 2012).

[17] T. Li, H. Lu, L. Fu, H. H. Tan, C. Jagadish, and M. Dagenais, "Enhanced Carrier Collection Efficiency and Reduced Quantum State Absorption by Electron Doping in Self-Assembled Quantum Dot Solar Cells," Appl. Phys. Lett. 106, 053902 (February 2015).

[18] R. Oshima, A. Takata, Y. Shoji, K. Akahane, Y. Okada, "InAs/GaNAs strain-compensated quantum dots stacked up to 50 layers for use in high-efficiency solar cell," Physica E 42, 2757–2760 (September 2010).

[19] R. B. Laghumavarapu, M. Sun, P. J. Simmonds, B. Liang, S. Hellstroem, Z. Bittner, S. Polly, S. Hubbard, A. G. Norman, J-W. Luo, R. Welser, A. K. Sood, and D. L. Huffaker, "New Quantum Dot Nanomaterials to Boost Solar Energy Harvesting," SPIE Newsroom 10.1117/2.1201401.005315 (January 2014).

[20] R. E. Welser, A. K. Sood, R. B. Laghumavarapu, D. L. Huffaker, D. M. Wilt, N. K. Dhar and K. A. Sablon, "The Physics of High-Efficiency Thin-Film III-V Solar Cells," Solar Cells - New Approaches and Reviews, L. A. Kosyachenko (Ed.), InTech, DOI: 10.5772/59283 (October 2015).

[21] L. C. Hirst, R. J. Walters, M. F. Fuhrer, and N. J. Ekins-Daukes, "Experimental Demonstration of Hot-Carrier Photo-Current in an InGaAs Quantum Wells Solar Cell," Appl. Phys. Lett. vol. 104, no. 061902 (June 2014).

[22] J. Tang, V. R. Whiteside, H. Esmaielpour, S. Vijeyaragunathan, T. D. Mishima, M. B. Santos, and I. R. Sellers, "Effects of Localization on Hot Carriers in InAs/AlAs$_x$Sb$_{1-x}$ Quantum Wells," Appl. Phys. Lett., vol. 106, no. 061902 (February 2015).

[23] A. Le Bris and J.-F. Guillemoles, "Hot Carrier Solar Cells: Achievable Efficiency Accounting for Heat Losses in the Absorber and Through Contacts," Appl. Phys. Lett., vol. 97, no. 113506 (September 2010).

[24] L. C. Hirst, H. Fujii, Y. Wang, M. Sugiyama, and N. J. Ekins-Daukes, "Hot Carriers in Quantum Wells for Photovoltaic Efficiency Enhancement," IEEE J. of Photovoltaics, vol. 4, pp. 244-252 (January 2014).

[25] H. Esmaielpour, V.R. Whiteside, J. Tang, S. Vijeyaragunathan, T. D. Mishima, S. Cairns, M. B. Santos, B. Wang, I. R. Sellers, "Suppression of phonon-mediated hot carrier relaxation in type-II InAs/AlAs$_x$Sb$_{1-x}$ quantum wells: a practical route to hot carrier solar cells," Progress in Photovoltaics, accelerated publication (February 2016).

[26] R. E. Welser, A. K. Sood, S. R. Tatavarti A. Wibowo, D. M. Wilt and A. Howard, "Radiative Dark Current in Optically-Thin III-V Photovoltaic Devices," Proc. of SPIE, vol. 9358, no. 93580Q (February 2015).

[27] A.G. Aberle, S. R. Wenham, and M. A. Green, "A New Method for Accurate Measurements of the Limped Series Resistance of Solar Cells," Proceedings of the 23rd IEEE Photovoltaic Specialists Conference, pp. 133-139 (May 1993).

[28] Y. Okada, N. Shiotsuka, and T. Takeda "Potentially Modulated Multi-Quantum Wells for High-Efficiency Solar Cell Applications," Solar Energy Materials & Solar Cells, vol. 85, pp. 143-152 (June 2005).

[29] Y. Okada and N. Shiotsuka, "Fabrication of Potentially Modulated Multi-Quantum Well Solar Cells," Proceedings of the 31st IEEE Photovoltaic Specialists Conference, p.p. 591-594 (December 2005).

[30] R. E. Welser, O. A. Laboutin, M. Chaplin, and V. Un, "Reducing Non-Radiative and Radiative Recombination in InGaAs Quantum Well Solar Cells," Proceedings of the 37th IEEE Photovoltaic Specialists Conference, 002683-002686 (June 2011).

[31] Y. Wen, Y. Wang, K. Watanabe, M. Sugiyama, and Y. Nakano "Effect of GaAs Step Layer on InGaAsGaAsP Quantum Well Solar Cells," Applied Physics Express, vol. 4, no. 122301 (November 2011).

[32] Y. Wang, H. Sodabanlu, S. Ma, H. Fujii, K. Watanabe, M. Sugiyama, and Y. Nakano "A Multi-Step Superlattice Solar Cell with Enhanced Subband Absorption and Open Circuit Voltage," Proceedings of the 38th IEEE Photovoltaic Specialists Conference, p.p. 001940 - 001943 (June 2012).

[33] Y. Takeda and T. Motohiro, "Hot-Carrier Extraction from Intermediate-Band Absorbers through Quantum-Well Energy-Selective Contacts," Jap. J, Applied Physics 51, 10ND03 (October 2012).